

Intermittent spatial chaos in the polarization of counterpropagating beams in a birefringent optical fiber

S. Trillo* and S. Wabnitz

Fondazione Ugo Bordoni, Viale Europa 190, 00144 Rome, Italy

(Received 23 March 1987)

Two counterpropagating intense light beams linearly polarized along the fast axis of a birefringent fiber may constitute a spatially unstable polarization eigenarrangement. Chaotic behavior in the steady-state polarization evolution of the waves occurs for input powers in a certain interval of values. By evaluating Lyapunov exponents we show intermittent trapping of irregular trajectories around regular islands. The characteristic length scale of this spatial disorder is typically of the order of one beat length.

The field of instabilities and chaos in nonlinear optical media has been rapidly growing over the past years.¹ It has been recently discovered that the coherent coupling between *copropagating* waves in a nonlinear medium may originate spatially unstable nonlinear eigensolutions.²⁻⁷ Predicted self-switching of the polarization state at the output of a birefringent fiber has been recently experimentally observed by raising the input power across the instability threshold.⁶ In the presence of longitudinal inhomogeneities such as periodic perturbations to the fiber birefringence, the coupling is modeled by a nonautonomous one-degree-of-freedom nonlinear system which exhibits chaos.⁷

In this work we consider two arbitrarily polarized intense beams *counterpropagating* in a birefringent Kerr-type medium. On traversal through an isotropic Kerr medium, beams of different intensity and linearly polarized along the same direction (or constituting a nonlinear *eigenpolarization arrangement*⁸) experience a power-dependent nonreciprocal phase shift.⁹⁻¹¹ This may substantially affect the operation of devices such as fiber-optic gyroscopes.¹² For beams possessing a generic input polarization state, field components along orthogonal axes suffer different nonlinear retardations, which entails nonreciprocal polarization changes.¹³ For nonbirefringent media, it has been shown that this effect

may induce an intrinsic spatial instability in the collinear degenerate four-wave-mixing (DFWM) process.^{2,13}

In a monomode fiber, unavoidable deviations from circularity of the core or external perturbations such as winding on a coil lift the ideal degeneracy in the propagation constants of two orthogonal linearly polarized (low-power) eigenmodes, and a relatively weak linear birefringence results. In order to overcome the resulting light depolarization, a dominant birefringence with well-defined principal axes can be directly built into the fiber. Consider the effect of a slight misalignment from the fiber axes of two counterpropagating waves linearly polarized at the respective input ends. The linear phase shift between the modes combines itself with a self-induced ellipse rotation¹⁴ and an additional nonlinear birefringence due to the counterpropagating wave.¹³ We show how, for a critical range of input powers, the competition of these effects may lead to spatial disorder in the polarization state of the waves, even for equally intense beams. Abrupt transition from quasiperiodic to chaotic (and vice versa) evolutions may occur after an unpredictable distance. To our knowledge, this is the first example of spatial intermittency.

The total electric field (at optical frequency ω_0) along the propagation distance z can be written as

$$\mathbf{E}(\mathbf{r}, z, t) = \sum_{j=1}^2 \{ E_{jx}(z) \exp[-i(-1)^j \beta_x z] \mathbf{x} + E_{jy}(z) \exp[-i(-1)^j \beta_y z] \mathbf{y} \} f(\mathbf{r}) \exp(-i\omega_0 t). \quad (1)$$

We denote with $f(\mathbf{r})$ the common field distribution in the transverse (x, y) plane of the two nearly degenerate linear modes, with propagation constant β_x and β_y , respectively. The four waves in Eq. (1) are coupled by the third-order nonlinear polarizability¹⁴

$$\mathbf{P}^{(3)} = A(\mathbf{E} \cdot \mathbf{E}^*)\mathbf{E} + (B'/2)(\mathbf{E} \cdot \mathbf{E})\mathbf{E}^*, \quad (2)$$

where $A = 6\chi_{1212}(\omega_0; \omega_0, \omega_0, -\omega_0)$ and $B' = 6\chi_{1221}(\omega_0; \omega_0, \omega_0, -\omega_0)$. In the slowly-varying-envelope approximation, the mode amplitude $E_{1y}(E_{2y})$ obeys the system

$$\begin{aligned} i(-1)^j dE_{jy}/dz = R \{ & (|E_{jy}|^2 + 2|E_{(3-j)y}|^2)E_{jy} + (1-B/2)(|E_{jx}|^2 + |E_{(3-j)x}|^2)E_{jy} \\ & + BE_{jx}E_{(3-j)x}E_{(3-j)y}^* + (1-B/2)E_{jx}E_{(3-j)y}E_{(3-j)x}^* \exp[-i(-1)^j 2\Delta\beta z] \\ & + (B/2)E_{jx}^2 E_{jy}^* \exp[-i(-1)^j 2\Delta\beta z] \}, \end{aligned} \quad (3)$$

where $\Delta\beta = \beta_x - \beta_y$, $R = k_0 n_2 4\pi 10^7 / n_1 c A_{\text{eff}}$, n_2 (n_1) is the nonlinear (linear) refractive index, $A_{\text{eff}} = (\int f^2 dr)^2 / \int f^4 dr$, and $B = B' 12\pi / n_1 n_2$. The equations for the amplitudes E_{jx} are obtained from (3) by exchanging x with y and $\Delta\beta$ with $-\Delta\beta$ throughout. From Eqs. (3) one obtains that the powers in the two beams $P_1 \equiv E_{1x}^2 + E_{1y}^2$ and $P_2 \equiv E_{2x}^2 + E_{2y}^2$ are separately conserved. The existence of a third invariant of Eqs. (3) leads to showing that the polarization evolutions of the waves are generated by a two-degree-of-freedom Hamiltonian.¹⁵ Since we will be only concerned here into numerically investigating the stochasticity transition, we adopt the Stokes vector formalism,^{3,13} that allows for substantial reduction of complexity in the dynamic equations.

Rewriting Eq. (3) in terms of the Stokes parameters

$$\begin{aligned} S_0 &= |E_{1x}|^2 + |E_{1y}|^2, \quad S_1 = |E_{1x}|^2 - |E_{1y}|^2, \\ S_2 &= 2 \operatorname{Re}[E_{1x} E_{1y}^* \exp(i\Delta\beta z)], \\ S_3 &= 2 \operatorname{Im}[E_{1x} E_{1y}^* \exp(i\Delta\beta z)], \end{aligned} \quad (4)$$

and similarly associating W_0, W_1, W_2, W_3 with E_{2x} and E_{2y} , one obtains

$$\begin{aligned} dS_0/dz &= 0, \quad dW_0/dz = 0, \\ d\mathbf{S}/dz &= [\boldsymbol{\Omega}(\mathbf{S} + 2\mathbf{W}) + \boldsymbol{\Omega}_L] \times \mathbf{S}, \\ d\mathbf{W}/dz &= \mathbf{W} \times [\boldsymbol{\Omega}_L + \boldsymbol{\Omega}(\mathbf{W} + 2\mathbf{S})], \end{aligned} \quad (5)$$

with $\mathbf{S} \equiv (S_1, S_2, S_3)$, and $\mathbf{W} \equiv (W_1, W_2, W_3)$. Further, $\boldsymbol{\Omega}_L \equiv (\Delta\beta, 0, 0)$ represents linear birefringence, while $\boldsymbol{\Omega}(\mathbf{x}) \equiv (R/2)((1+B/2)x_1, (1+B/2)x_2, (1-3B/2)x_3)$ is associated with light-induced birefringence.

For low power beams, the only eigenpolarizations (i.e., the fixed points of Eqs. (5), defined by $d\mathbf{S}/dz = d\mathbf{W}/dz = 0$) are $\mathbf{S} = (\pm S_0, 0, 0)$ and $\mathbf{W} = (\pm W_0, 0, 0)$, which represent waves linearly polarized along fiber principal axes. Define the normalized powers $p_{1,2} \equiv P_{1,2}/P_c = R(1+B/2)P_{1,2}/2\Delta\beta$ and take $p_1 \geq p_2$. As

$$p_1 + p_2 \geq \frac{1}{2} \quad \text{and} \quad p_1 - p_2 \leq \frac{1}{2}, \quad (6)$$

the point $\mathbf{S} = (-S_0, 0, 0)$, $\mathbf{W} = (-W_0, 0, 0)$ become unstable and two new stable eigenarrangements of linearly polarized waves occur. The forward field is oriented at

$$\Theta_1 = \left(\frac{1}{2}\right) \tan^{-1}[(1-f^2)^{1/2}/f] \quad (7)$$

with respect to the fast axis, with $f \equiv p_1 - p_2^2/p_1 + 1/(4p_1)$. For the backward propagating beam, Θ_2 [obtainable from Eq. (7) by interchanging subscripts in f] is measured from the fast axis in the counterrotating direction with respect to Θ_1 . In particular, whenever $p_1 = p_2 \equiv p \equiv P/P_c$ the arrangement oriented along the fast axis bifurcates for $p > \frac{1}{4}$, and $|\Theta_1| = |\Theta_2| = \frac{1}{2} \tan^{-1}(16p^2 - 1)^{1/2}$. Taking $A_{\text{eff}} = 10^{-7} \text{ cm}^2$, $n_2 = 2 \times 10^{-13} \text{ esu}$, a beat length $L_b \equiv 2\pi/\Delta\beta = 5 \text{ m}$, and $\lambda = \omega/2\pi c = 1 \mu\text{m}$, bifurcation occurs for $P = 14 \text{ W}$ coupled to a silica [$B = \frac{2}{3}$ (Ref. 16)] monomode fiber. Notice that for a single beam polarized along the fast

axis polarization instability occurs for $p > (1+B/2)/2B$.²⁻⁶ For silica, this last condition reduces to $p \geq 1$, therefore observation of instability in the polarization of a single beam requires twice as much total power with respect to the case considered here.

As a consequence of this instability we will show that, even in the particularly symmetric case of equally intense beams, the solution of Eqs. (5) exhibits chaotic properties. We will focus our attention onto the relevant case $B = \frac{2}{3}$. Defining $\mathbf{s} \equiv \mathbf{S}/P$ and $\mathbf{w} \equiv \mathbf{W}/P$, Eq. (5) reduce in explicit form to

$$\begin{aligned} s'_1 &= ps_2 s_3 + 2ps_3 w_2, \\ s'_2 &= -ps_1 s_3 - 2ps_3 w_1 - s_3, \\ s'_3 &= 2p(s_2 w_1 - w_2 s_1) + s_2, \end{aligned} \quad (8)$$

where primes denote differentiation with respect to the distance $\xi \equiv \Delta\beta z$, and the derivatives for the w_i 's are obtainable from Eqs. (8) by exchanging the sign of the right-hand sides and s_i and with w_i everywhere.

In order to characterize the transition to stochasticity in the DFWM process, we estimated the maximal Lyapunov exponent λ_m which measures the exponential rate of divergence of nearby trajectories.¹⁷ From Eqs. (8) (and corresponding equations for the w_i 's) written as $dx_j/d\xi = f_j(\mathbf{x})$, $j = 1, \dots, 6$ one obtains the vector \mathbf{t} tangent to the six-dimensional evolution $\mathbf{x}(\xi)$ by integrating

$$dt_j/d\xi = \sum_{i=1}^6 (\partial f_j / \partial x_i) t_i, \quad i = 1, \dots, 6 \quad (9)$$

which yields the local maximal Lyapunov exponent

$$\lambda_m(\mathbf{Z}) \equiv (1/\mathbf{Z}) \ln[|\mathbf{t}(\mathbf{Z})|/|\mathbf{t}(0)|], \quad (10)$$

where $\mathbf{Z} = z/L_b = \xi/2\pi$. Figure 1 refers to the case of a normalized power $p = 0.5$, and illustrates the estimated values of $\lambda_m(\mathbf{Z})$ for five evolutions corresponding to

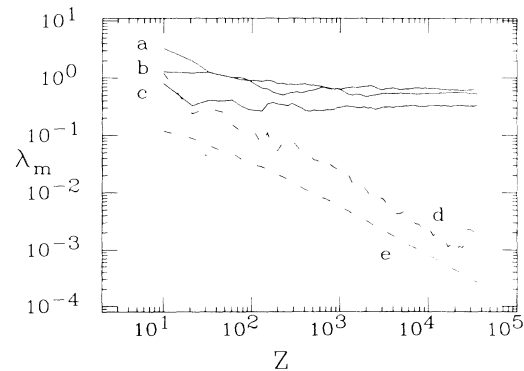


FIG. 1. Maximal Lyapunov exponents $\lambda_m(\mathbf{Z})$ vs $\mathbf{Z} = \xi/2\pi = z/L_b$ for different polarization states and $p = 0.5$. a, $[\mathbf{s}(0); \mathbf{w}(0)] = (-0.5, 0, 0.866; -0.5, 0, 0.866)$; b, $(-0.5, 0, 0.866; -0.4, 0, 0.917)$; c, $(-0.98, 0, 0.2; -0.98, 0.2, 0)$; d, $(-0.9999, 0.01, 0.01412; -0.9999, -0.01, 0.01412)$; e, $(0.95, 0.1, 0.296; 0.95, -0.1, -0.296)$.

different states of polarization $\mathbf{s}(0)$ and $\mathbf{w}(0)$ at the end face $Z=0$ of the fiber. As can be seen, stochastic (λ_m converges to positive values: cases *a*–*c* in Fig. 1) as well as ordered ($\lambda_m \rightarrow 0$ as $1/Z$: cases *d* and *e*) evolutions coexist at a certain fixed optical power of the beams. Therefore, onset of chaoticity in DFWM may simply depend upon the specific form of the reflectivity tensor of a mirror with 100% intensity reflection positioned at the fiber end face.

Figure 2 displays the power spectrum of the s_3 coordinate of trajectory *b* in Fig. 1. A highly irregular spatial frequencies content is superimposed onto a linear decay, a behavior that is typical of chaotic solutions. Determining the scale of length for the exponential separation of the trajectories in the \mathbf{x} space is of primary physical relevance. In fact, this distance sets a fundamental limit to the length of a fiber since the chaotic exchange of power between the fiber axes could spoil the operation of a fiber-based four-wave mixer. Figure 3 shows Lyapunov exponents, computed using different p and a fixed choice of polarizations at $z=0$. As can be seen, the characteristic scale for chaos (defined as $z_c \equiv L_b/\lambda_m$) decreases as p grows larger, ranging from $z_c = 1.4L_b$ for $p = \frac{1}{2}$ down to $z_c = 0.7L_b$ at powers $p > 2$. In practice, the instability could be observable using short fibers (of length $\cong z_c$) if the threshold power for competing nonlinear effects [such as stimulated Brillouin scattering (SBS) induced by an individual beam] were higher than P_c . For the typical fiber parameters given above, a sample of length $L = 30$ cm and a laser bandwidth of 1 GHz, the SBS threshold is $P_b = 400$ W.¹⁸ This power yields $p = 0.5$ using $L_b = 26$ cm (so that $L/L_b \cong z_c/L_b$). Polarization chaos becomes the lower threshold power nonlinear effect (also using longer fibers or spectrally narrower sources) when using SBS suppression (e.g., by means of a thermal gradient^{18,19}).

As can be seen from Fig. 3, the trajectory becomes chaotic just above $p > \frac{1}{4}$ and is regular once again for $p > 3$, owing to the fact that the nonlinear birefringence quenches the linear one. At sufficiently high powers, al-

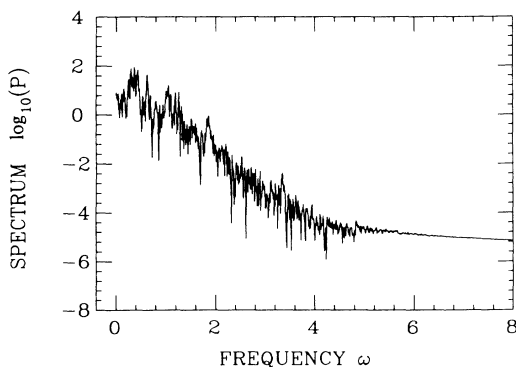


FIG. 2. Log power spectrum against spatial frequency $\omega = 2\pi/\xi$ from a 2^{13} -points fast Fourier transform of the s_3 component of trajectory *b* in Fig. 1 over the interval $0 \leq Z \leq 128$.

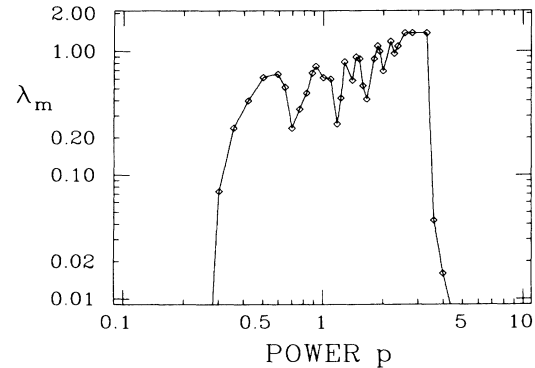


FIG. 3. Lyapunov exponents $\lambda_m(Z)$ vs power p for initial conditions as in case *b* of Fig. 1.

most all of the chaotic trajectories get trapped by regular Kolmogorov-Arnol'd-Moser (KAM) tori, topologically equivalent to those of an isotropic medium [Eqs. (5) integrable as $\Delta\beta/R \rightarrow 0$ (Ref. 13)].

Figure 4 shows the evolution of s_3 as extracted from trajectory *a*, as it would be obtained by placing at $Z=0$ an ideal metallic mirror [i.e., only the propagation direction and therefore the wave handedness is reversed in sign upon reflection, with no change in eccentricity of the polarization ellipse: $s_1(0)=w_1(0)$, $s_2(0)=w_2(0)$, and $s_3(0)=w_3(0)$]. The polarization state, initially trapped along an invariant torus, suddenly evolves in an erratic way. This intermittency does not stem from numerically generated noise, but rather constitutes a universal feature common to a wide class of nonlinear area-preserving systems and maps: See, for example, the Ulam map²⁰ (associated with the Fermi acceleration of cosmic rays).

Figure 5 illustrates the fact that a single polarization trajectory may alternately get captured along a KAM torus, corresponding a Z^{-1} slope for the Lyapunov exponent, and then escape into chaos for an essentially unpredictable distance. Since most of the computed evo-

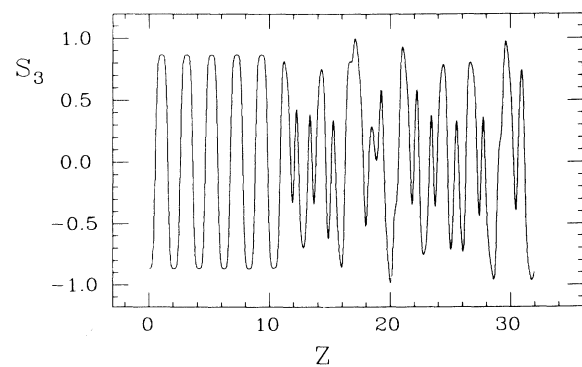


FIG. 4. Evolution of s_3 as in case *a* of Fig. 1, against $Z = \xi/2\pi$.

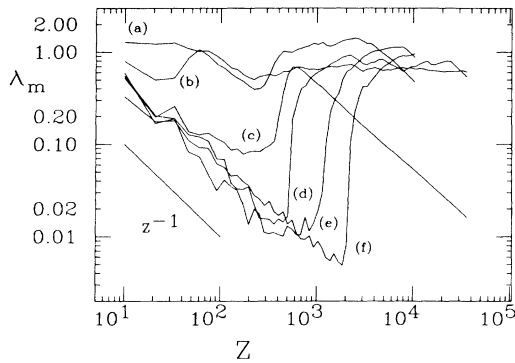


FIG. 5. $\lambda_m(Z)$ vs Z for initial polarization as in case *b* of Fig. 1, and different powers. (a), $p=1$; (b), $p=3.31$; (c), $p=4$; (d), $p=2$; (e), $p=3.047$; (f) $p=2.272$.

lutions exhibit the intermittent trapping phenomenon as $p > 2$, in Fig. 3 we reported maximal Lyapunov exponents relative to the chaotic subsections only [e.g., estimated from the top of the bumps in cases *e* and *f* of Fig. 5].

Suppose that one slightly varies in the stochasticity interval the power of an intense light beam launched into a fiber and mirror combination. Abrupt switching of the

intensity of one polarization component (detected beyond an analyzer) of the back-reflected wave should be expected as observable consequence of the exponential separation along the fiber sample of nearby polarization trajectories.⁷

It is interesting to point out that scalar models for counterpropagating fields in nonlinear distributed feedback structures predict flat plateaus of the transmitted intensity as a function of the incident intensity, an effect originating from spatially chaotic or unstable solutions.²¹ Extensions to the vectorial case which has been treated in the present work is under investigation and will be reported elsewhere.

Finally, as the temporal dependence of the field envelopes and the nonzero medium response time are accounted for, temporal instabilities of the output intensities may occur even for the spatially stable eigenarrangements.^{22,23} A still open issue is the analysis of the regimes of spatiotemporal turbulence.

We gratefully acknowledge many valuable suggestions by A. Vulpiani. We thank R. W. Boyd for sending copies of his work prior to publication. This work was carried out under an agreement between the Fondazione Bordonni and the Istituto Superiore Poste e Telecomunicazioni.

*Also with Dipartimento di Fisica, Università degli Studi di Roma I, P. Moro 2, 00185 Rome, Italy.

¹See *Optical Instabilities*, edited by R. W. Boyd *et al.* (Cambridge University Press, Cambridge, England, 1986).

²J. Yumoto and K. Otsuka, *Phys. Rev. Lett.* **54**, 1806 (1985).

³B. Daino, G. Gregori, and S. Wabnitz, *J. Appl. Phys.* **58**, 4512 (1985); B. Daino, G. Gregori, and S. Wabnitz, *Opt. Lett.* **11**, 42 (1986); G. Gregori and S. Wabnitz, *Phys. Rev. Lett.* **56**, 600 (1986).

⁴H. G. Winful, *Opt. Lett.* **11**, 33 (1986).

⁵F. Matera and S. Wabnitz, *Opt. Lett.* **11**, 467 (1986); S. Trillo and S. Wabnitz, *Appl. Phys. Lett.* **49**, 752 (1986); S. Wabnitz, E. W. Wright, C. T. Seaton, and G. I. Stegeman, *ibid.* **49**, 838 (1986); A. Mecozzi, S. Trillo, S. Wabnitz, and B. Daino, *Opt. Lett.* **12**, 275 (1987).

⁶S. Trillo, S. Wabnitz, R. H. Stolen, G. Assanto, C. T. Seaton, and G. I. Stegeman, *Appl. Phys. Lett.* **49**, 1224 (1986).

⁷S. Wabnitz, *Phys. Rev. Lett.* **58**, 1415 (1987).

⁸Polarized at the respective fiber input ends so that they maintain their state of polarization unchanged.

⁹R. Y. Chiao, P. L. Kelley, and E. Garmire, *Phys. Rev. Lett.* **17**, 1198 (1966).

¹⁰A. E. Kaplan and P. Meystre, *Opt. Lett.* **6**, 590 (1981).

¹¹A. E. Kaplan, *Opt. Lett.* **8**, 560 (1983).

¹²R. A. Bergh, H. C. Lefevre, and H. J. Shaw, *Opt. Lett.* **7**, 282 (1982).

¹³S. Wabnitz and G. Gregori, *Opt. Commun.* **59**, 72 (1986).

¹⁴P. D. Maker, R. W. Terhune, and C. M. Savage, *Phys. Rev. Lett.* **12**, 507 (1964); note that, owing to their relatively weak birefringence [$\delta n \equiv (\beta_x - \beta_y)\lambda/2\pi \cong 10^{-5} - 10^{-6}$], isotropic third-order susceptibility is generally assumed for optical fibers.

¹⁵E. Caglioti, S. Trillo, and S. Wabnitz (unpublished).

¹⁶A. Owyong, R. W. Hellwarth, and N. George, *Phys. Rev. B* **5**, 628 (1972).

¹⁷G. Benettin, L. Galgani, and J. M. Strelcyn, *Phys. Rev. A* **14**, 2338 (1976).

¹⁸R. H. Stolen, *Proc. IEEE* **68**, 1232 (1980).

¹⁹M. D. Levenson, M. R. Shelby, M. D. Reid, D. F. Walls, and A. Aspect, *Phys. Rev. A* **32**, 1550 (1985).

²⁰A. J. Lichtenberg and M. A. Lieberman, *Regular and Stochastic Motion* (Springer-Verlag, New York, 1983), Chap. 3, p. 190; V. Merlo, M. Pettini, and A. Vulpiani, *Lett. Nuovo Cimento* **44**, 163 (1985).

²¹F. Delyon, Y. E. Lévy, and B. Souillard, *Phys. Rev. Lett.* **57**, 2010 (1986); A. Mecozzi, S. Trillo, and S. Wabnitz, *Opt. Lett.* (to be published).

²²Y. Silberberg and I. Bar-Joseph, *Phys. Rev. Lett.* **48**, 1541 (1982).

²³A. L. Gaeta, R. W. Boyd, J. R. Ackerhalt, and P. W. Milonni, *Phys. Rev. Lett.* **58**, 2432 (1987).